

---

# Microstructure Modelling in Additive Manufacturing

---

## DISSERTATION REPORT

*Submitted in partial fulfillment of the requirements of  
BITS G540 Dissertation*

*By*

Pushkar Anirudha PANDIT  
ID No. 2018H1060216P

*Under the supervision of:*

Dr. Murali PALLA



BIRLA INSTITUTE OF TECHNOLOGY AND SCIENCE PILANI, PILANI CAMPUS

June 2020

# Certificate

This is to certify that the report entitled, “*Microstructure Modelling in Additive Manufacturing*” and submitted by Pushkar Anirudha PANDIT ID No. 2018H1060216P in partial fulfillment of the requirements of BITS G540 Dissertation embodies the work done by him under my supervision.

---

*Supervisor*

Dr. Murali PALLA

Asst. Professor,

BITS-Pilani Pilani Campus

Date:

# *Acknowledgements*

I would like to express my sincere gratitude to my advisor Dr. Murali PALLA. Asst. Professor, Department of Mechanical Engineering, BITS-Pilani Pilani Campus for providing his invaluable guidance , comments and suggestions throughout the course of the Dissertation.

Apart from my advisor, I would like to show gratitude towards Dr. M.S Dasgupta , Head of Department, Department of Mechanical Engineering for providing with the timely guidance to pursue thesis which lead to this work .

Lastly, I wish to thank my colleagues in Mechanical Department for their timely suggestions on my thesis work and significantly I thank Swapnil Bhure (2017-2019), graduate student in Mechanical Department for providing his useful suggestions on thesis and simulation part of the work.

BIRLA INSTITUTE OF TECHNOLOGY AND SCIENCE PILANI, PILANI CAMPUS

## *Abstract*

Masters in Engineering(Mech.)

### **Microstructure Modelling in Additive Manufacturing**

by Pushkar Anirudha PANDIT

With the ongoing efforts in materials community to address the very manufacture of sustainable components with AM, various attempts are being made to co relate the process parameters with micro structural description of the material along with significant efforts to simulate the same. In this attempt, the thesis tries to understand the current scenario in this context with an adequate literature review and build upon the basics of materials modelling so as to equip enough to carry forward these simulations to AM.

# Contents

<b>Certificate</b>	<b>i</b>
<b>Acknowledgements</b>	<b>ii</b>
<b>Abstract</b>	<b>iii</b>
<b>Contents</b>	<b>iv</b>
<b>Abbreviations</b>	<b>v</b>
<b>1 Theoretical Background</b>	<b>1</b>
1.1 Thermodynamics of Solid Solutions . . . . .	1
1.2 Diffusion . . . . .	7
1.3 Solidification . . . . .	10
1.4 Classical Theory of Nucleation . . . . .	11
<b>2 Literature Survey</b>	<b>13</b>
2.1 Introduction . . . . .	13
2.2 Literature Review . . . . .	13
<b>3 Computational Approaches</b>	<b>16</b>
3.1 Cellular Automata Method . . . . .	17
3.2 Phase Field(PF) Method . . . . .	19
3.2.1 Cahn-Hilliard Treatment of Spinodal Decomposition . . . . .	20
3.3 Monte Carlo Methods . . . . .	20
3.3.1 Ising Model . . . . .	21
3.3.2 Kinetic Monte Carlo . . . . .	23
3.4 Needle Network Method . . . . .	26
<b>Bibliography</b>	<b>27</b>

# Abbreviations

<b>CA</b>	Cellular Automata
<b>MAM</b>	Metal Additive Manufacturing
<b>DED</b>	Directed Energy Deposition
<b>PBF</b>	Powder Bed Fusion
<b>WAAM</b>	Wire Arc Additive Manufacturing
<b>AM</b>	Additive Manufacturing
<b>PSP</b>	Process-Structure-Property
<b>PF</b>	Phase Field
<b>kMC</b>	Kinetic Monte Carlo
<b>EBSD</b>	Electron Back Scatter Diffraction
<b>2D</b>	Two Dimensional
<b>DNN</b>	Dendritic Needle Network

# Chapter 1

## Theoretical Background

In an attempt to understand the micro structure evolution during additive manufacturing which stems from a sound understanding of phase transformations in alloys, a comprehensive study of these transformations in metals and alloys was conducted. While gaining insights from the different phenomenon an attempt has been made to stay consistent with the big picture in mind to model microstructure and explore the appropriate underlying phenomenon to grasp the necessary pre requisite knowledge for the same. This study starts off with a concrete knowledge of thermodynamics of solutions precisely solid solutions.

### 1.1 Thermodynamics of Solid Solutions

Thermodynamics becomes an essential tool to determine the state of equilibrium for any alloy. While chalking out a phase diagram one is always concerned about the changes that lead to this equilibrium. Before going on any further, a phase as defined in the literature can be attributed to a portion of a system whose properties and composition remain at equilibrium and retains its uniqueness when compared to other parts of the system. As can be suspected the reason for transformation is that the alloy in its initial state is relatively unstable to its final state to which it transforms. This stability of phases can be determined with the help of Gibbs free energy ( $G$ ) of the system at constant temperature and pressure as expounded by thermodynamics.

The classical thermodynamics also leads us to the result that a closed system at constant temperature and pressure achieves stable state which eventually becomes an equilibrium state at

a stage when its gibbs free energy attains the lowest possible value i.e.  $dG = 0$ . Apart from this stable state another state is observed which certainly satisfied the above discussed criteria but does not possess the lowest value when looked upon globally which is often called as a metastable state. Moreover, the states which lead to this stable equilibrium state are in fact unstable and are realised only momentarily during the course of the process. So, in effect the atoms when find themselves in these intermediate states do rearrange themselves to attain a global minima.

In order to understand the driving force for solidification for a single component alloy, the applicability of gibbs free energy proves to be quite essential. In order to understand the change

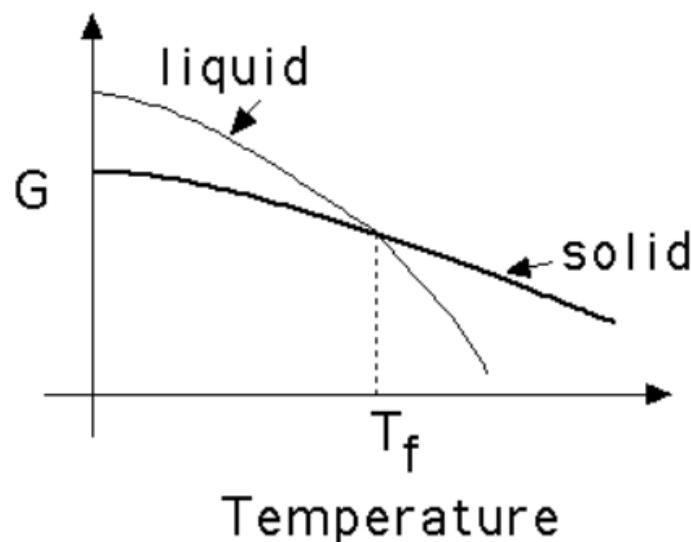


FIGURE 1.1: Driving Force for Solidification.

in phase during transformations in an alloy system demands an appreciation of how Gibbs energy of a phase depends on composition as well as temperature and pressure.

In an attempt to quantify the gibbs free energy of the alloy or rather a binary solution (for simplicity), it is assumed that both the species have same crystal structure which after mixing in certain proportions make a solid solution with same structure.

The Gibbs free energy of an assembly of both species before mixing needs to be determined in order to estimate the change in free energy of the solid solution after mixing as evident from the below figure.



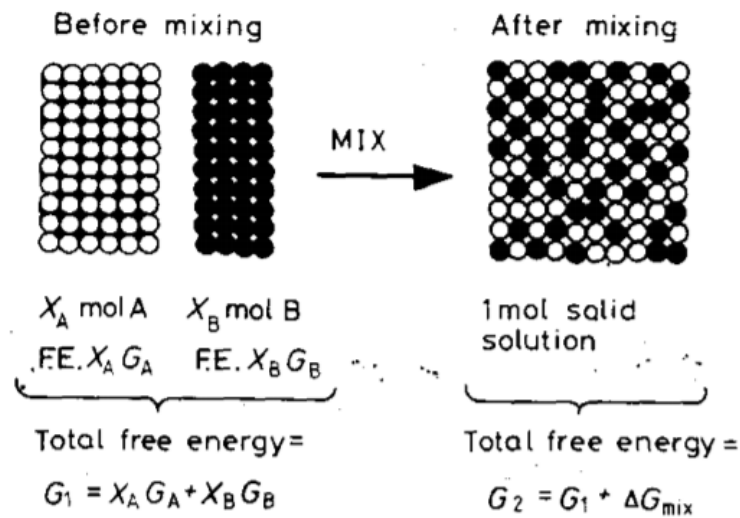


FIGURE 1.2: Free Energy of Mixing.Reprinted from [14]

From the simplicity point of view , model of ideal solution is treated first which encapsulates the assumption that the energy change during mixing is only due to change in entropy specifically due to configurational entropy and thermal entropy does not play any role in the change of energy if there is no change in volume or heat content during mixing. So, the change in Gibbs free energy can be expressed as

$$\Delta G_{\text{mix}} = RT(X_A \ln X_A + X_B \ln X_B)$$

which can be pictorially represented as

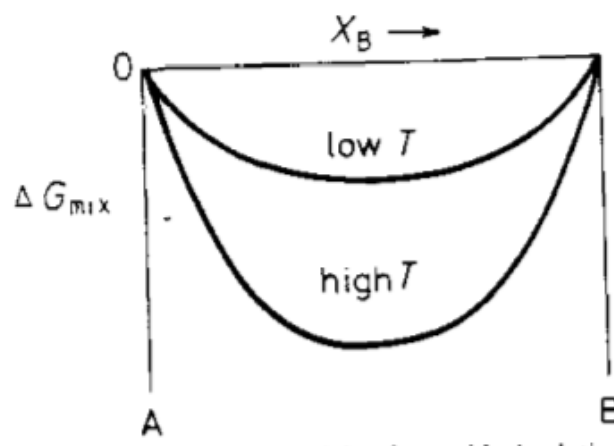


FIGURE 1.3: Free Energy of Mixing for an ideal Solution.Reprinted from [14]

Effectively, the total Gibbs free energy of an ideal solution can be expressed as

$$G = X_A G_A + X_B G_B + RT(X_A \ln X_A + X_B \ln X_B)$$

In case of alloys, it catches one's interest to figure out how this free energy changes when atoms are added or removed. This change in Gibbs Free energy can be quantitatively attributed to the derivative of Gibbs energy with respect to composition which is often known as **chemical potential** and is expressed as -

$$\mu_A = \left( \frac{\partial G}{\partial n_A} \right)_{T,P,n_B}$$

Another model that is relatively practical than the ideal solution model is Regular solution model which attempts to quantitatively account for the energy of mixing using a quasi chemical approach which assumes that the heat of mixing is only due to the bond energies between adjacent atoms. Here, the bond energy of mixing can be represented as

$$\epsilon = \epsilon_{AB} - \frac{1}{2}(\epsilon_{AA} + \epsilon_{BB})$$

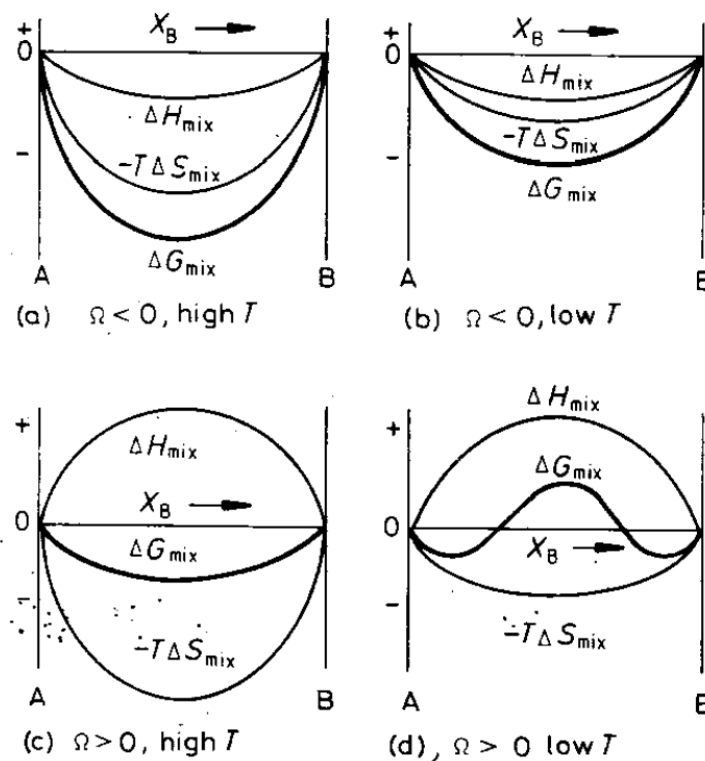
where  $\epsilon_{AB}$  is the energy associated with A-B bonds and  $\epsilon_{AA}, \epsilon_{BB}$  are similarly associated with A-A and B-B bonds respectively. Considering the number of bonds, the accumulative expression of enthalpy of mixing for the case when the above change in energy is not deviating much from zero can be expressed as -

$$\Delta H_{mix} = \Omega X_A X_B$$

where  $\Omega = N_a z \epsilon$  and  $z$  is the number of bonds per atom or to say coordination number. Moreover, if  $\epsilon < 0$  then the atoms in the solution will tend to be surrounded by opposite type of atoms and vice versa. Eventually the Gibbs free energy of mixing can be rewritten as -

$$\Delta G_{mix} = \Omega X_A X_B + RT(X_A \ln X_A + X_B \ln X_B)$$

The above expression when plotted for different values of  $\omega$  can be seen as -

FIGURE 1.4: Effect of  $\Delta H_{mix}$  and  $T$  on  $\Delta G_{mix}$ . Reprinted from [14]

Apart from chemical potential, an attempt can be made to relate the Gibbs Free Energy of A rich and B rich solution with their corresponding chemical potentials at equilibrium in the solution using another parameter known as **activity** which can be formulated or expressed as -

$$\mu_A = G_A + RT \ln a_A; \mu_B = G_B + RT \ln a_B$$

which varies with the composition of the solution. For a dilute solution of B in A, the activity coefficient i.e.  $\gamma_A = a_A/X_A$  one can observe a seen behaviour that is given by **Henry's Law** when  $\gamma_B \approx \text{const.}$  and **Raoult's Law** when  $\gamma_A \approx 1$ . So, to get a bigger picture activity and chemical potential are simply a measure of the tendency of atom to leave the solution.

Although the above model attempts to capture real systems by accounting for enthalpy of mixing but its utility is quite limited. As a primary observation, the systems in which  $\epsilon < 0$  leads to ordering of atoms to minimise its energy while the systems wherein  $\epsilon > 0$  the atoms tend to form clusters of A rich and B rich groups. However, this ordering or clustering will decrease as temperature increases due to the increasing importance of entropy. Also, when the difference in size of both the species is large enough then interstitial solid solutions are relatively more favourable energetically.

Apart from above discrepancies, in real system often the crystal structure of A and B are different in their respective pure states at a given temperature. Such cases are investigated for equilibrium by drawing two separate Gibbs free energy curve for each structure and the equilibrium compositions are determined by drawing a **common tangent** to both the curves and the state in region between these two compositions tends to separate into two phases of equilibrium composition i.e. the configuration always comes down the hill in the region between equilibrium compositions. As an visual effort to understand the above phenomenon can be represented as -

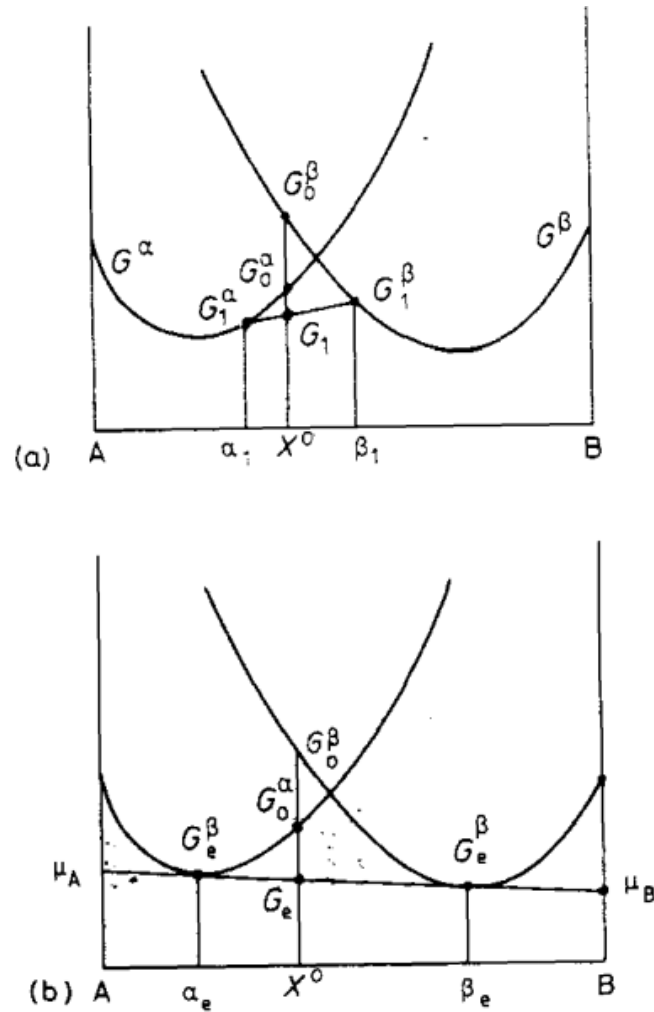


FIGURE 1.5: Free energy of a mixture. Reprinted from [14]

Quantitatively the above figure can be rewritten as -

$$\mu_A^\alpha = \mu_A^\beta, \mu_B^\alpha = \mu_B^\beta$$

## 1.2 Diffusion

The prime reason behind occurrence of diffusion which is an atomic phenomenon is to produce a decrease in Gibbs Free Energy . Diffusion ceases to occur when the chemical potentials of all atoms are same everywhere the the system reaches a state of equilibrium. In a crystalline solid with uniform concentration gradient this diffusion can be quantitatively expressed with a relationship between mass flux and concentration gradient as -

$$J_{net} = -D\nabla C$$

This mathematical statement is often called **Fick's First Law**.

At times we often face non uniform concentration gradients in practical situations so a relationship was established between time rate of change in concentration and its variation in space which eventually came to be known as **Fick's Second Law** and can be mathematically written as -

$$\frac{\partial C}{\partial t} = \nabla^2 C$$

Various phenomenon like carburisation and decarburisation can be studied with above set of partial differential equations .

Atoms in solid state often migrate by jumping into vacancies which can be either interstitial vacancy or substitutional vacancy. Since there are relatively larger number of interstitial vacancies at equilibrium when compared to substitutional vacancies, so interstitial atoms move quite faster than the substitutional solutes.

Often defects are found in non equilibrium concentrations in physical crystals. These defects certainly enhance the process of diffusion through certain paths. Thus, the diffusion that occurs through these defects such as grain boundaries is relatively much faster when compared with that in a perfect crystal. But, these defects do occupy a lesser fraction of composition as temperature increases which certainly affects its relative significance at higher temperatures as compared to that through the lattice. A rational qualitative explanation of diffusion can be anticipated when it is associated with the change in Gibbs free energy rather than concentration gradient. This can be quantitatively represented as -

$$J_A = -C_A M_A \nabla \mu_A; D_A = C_A M_A \frac{\partial \mu_A}{\partial C_A}$$

This relation certainly accounts for diffusion up as well as down the free energy hill.

A homogeneous solution when cooled in **miscibility region (curve ad)** reduces its gibbs free energy by decomposing into A-rich and B-rich atoms. This transformation is even enhanced when cooled within chemical **spinodal region (curve bc)** as the solution when cooled becomes unstable to changes in composition leading to separation of A rich and B rich atoms. Also if the solution happens to cool down in a region between miscibility gap and chemical spinodal then large perturbations in composition are needed for phase separation which is often achieved by **nucleation and growth**.

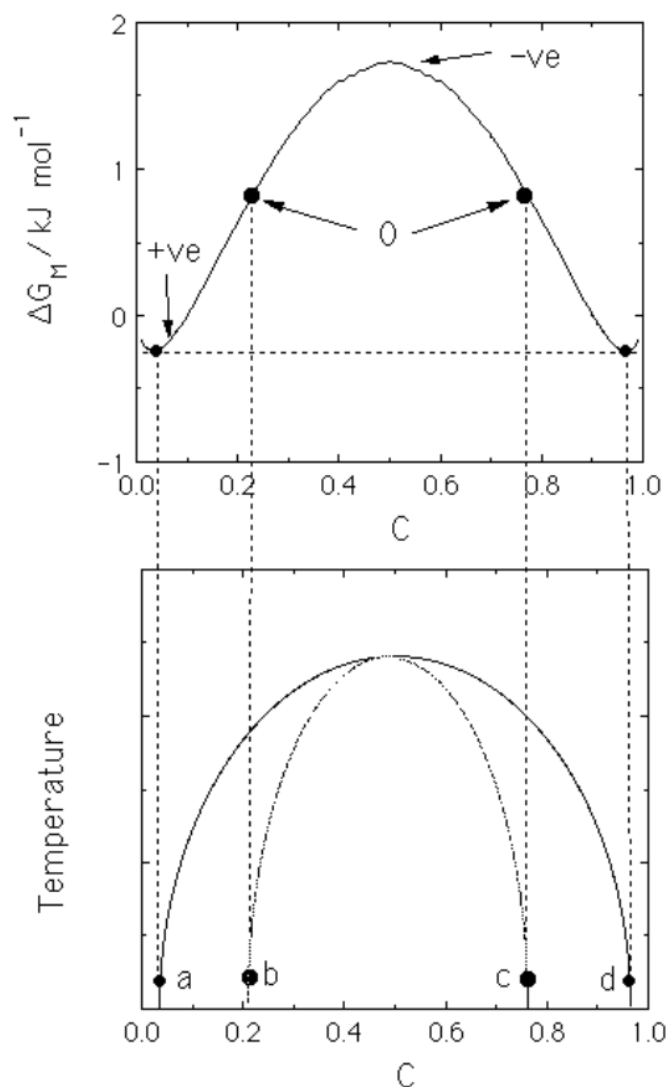


FIGURE 1.6: Miscibility gap and Chemical Spinodal. Reprinted from [5]

Phase separation inside spinodal region and that outside it can be appreciated with the following figure .

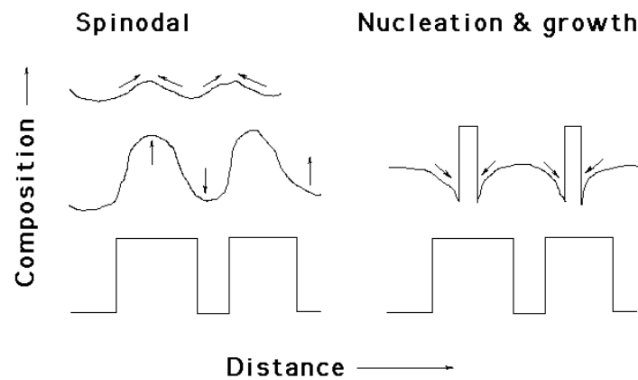


FIGURE 1.7: Uphill and Downhill diffusion. Reprinted from [5]

Practically this fluctuation in concentration eventually increases the coherency strain energy of the system which opposes the very phenomenon of uphill diffusion and a larger undercooling is required for spinodal decomposition or its occurrence can be traced if the solution lies under coherent spinodal region which is illustrated in following figure.

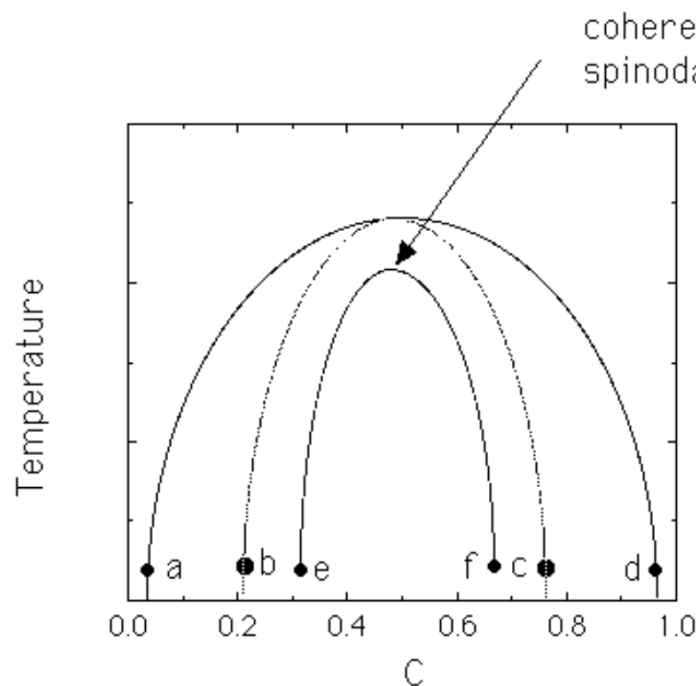


FIGURE 1.8: Coherent Spinodal. Reprinted from [5]

Another factor which can be anticipated to oppose this uphill diffusion is discrepancy in the Gibbs energy of non homogeneous system when compared to homogeneous solution which often

arises due to presence of interfaces in heterogeneous solution.

The growth or motion of interface is observed to be controlled by two mechanisms that is diffusion controlled motion and a interface controlled motion which occur simultaneously with varying extents in practical alloys. Diffusion controlled motion of interface is characterised by dissipation of much of energy by diffusion when compared to other phenomenon. Interface controlled growth occurs when much of the driving force is exhausted in process of transferring atoms across the interface. Moreover, this diffusion control motion of the interface eventually ceases its own growth as the solute diffuses over larger distances which can be quantitatively anticipated using conservation of mass and balance of solute diffusion.

An interesting phenomenon of solute trapping is often observed when the interface controlled motion takes place. It occurs when the solute particles do not get opportunity to leave away the interface as the interface moves at a faster rate. Quantitatively, this can be realised by increase in chemical potential across the interface.

### 1.3 Solidification

When a pure metal cools down in a mould cavity, a chill zone is observed near the walls of the mould which consist of fine crystals which grow in a preferred direction into the melt as the heat is extracted by the mould called as **columnar grains**. In case when the liquid at the centre tends to be colder than its solidification temperature than the liquid near the wall, we observe nucleation in the melt itself which grow in all direction called as **equiaxed grains**. These different type of grain morphologies can be realised quantitatively by the nature temperature gradients.

Associated with these equiaxed grains is the instability that is often observed which tend to grow in preferred directions called as **thermal dendrites**. These instabilities arise as with any fluctuation in the interface of these equiaxed grains, the melt surrounding it tends to supercool to a greater extent.

Solidification in alloys starts with partitioning or pileup of solute into the liquid ahead of solidification front which eventually changes the liquidus temperature of the melt and a super cooled zone of liquid ahead of solidification is observed. This phenomenon came to be known as **constitutional super cooling** due to variation in composition across interface. This can be illustrated as



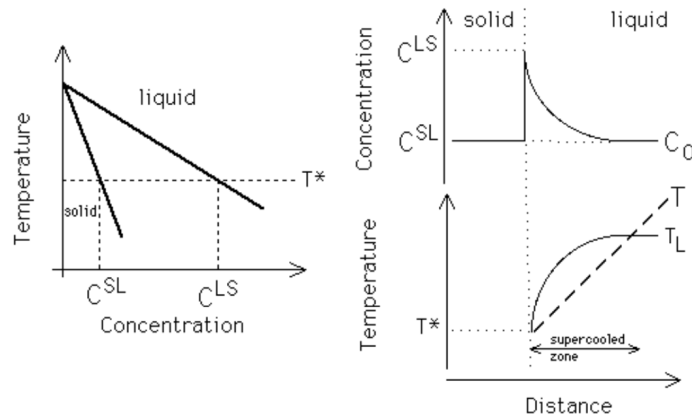


FIGURE 1.9: Constitutional Supercooling. Reprinted from [5]

This constitutional supercooling is the reason for growth into dendritic structures in alloys. Growth of planar interface into either cells or dendrites actually depends on the width of this supercooled zone. For smaller widths, cells develop and if these widths are wider relatively then dendrites develop from these planar interfaces.

## 1.4 Classical Theory of Nucleation

Fluctuations in phase often occur as random events because of thermal vibrations of atoms which may or may not be associated with reduction in free energy individually. In a metastable system, this leads to a critical size of fluctuation beyond which growth is favoured.

Considering a homogeneous nucleation of  $\alpha$  phase in  $\gamma$ . For a spherical particle of radius  $r$  with an isotropic interfacial energy  $\sigma_{\alpha\gamma}$ , the change in free energy is calculated as -

$$\Delta G = \frac{4}{3}\pi r^3 \Delta G_{CHEM} + \frac{4}{3}\pi r^3 \Delta G_{STRAIN} + 4\pi r^2 \sigma_{\alpha\gamma}$$

The variation in  $\Delta G$  with size of particle is given by -

$$\frac{\partial G}{\partial r} = 4\pi r^2 [\Delta G_{CHEM} + \Delta G_{STRAIN}] + 8\pi r \sigma_{\alpha\gamma}$$

The critical size needed for growth of a nuclei is calculated by setting the above derivative to 0.

$$r^* = -\frac{2\sigma_{\alpha\gamma}}{\Delta G_{CHEM} + \Delta G_{STRAIN}}$$

The variation in gibbs energy required for growth can be realised graphically as

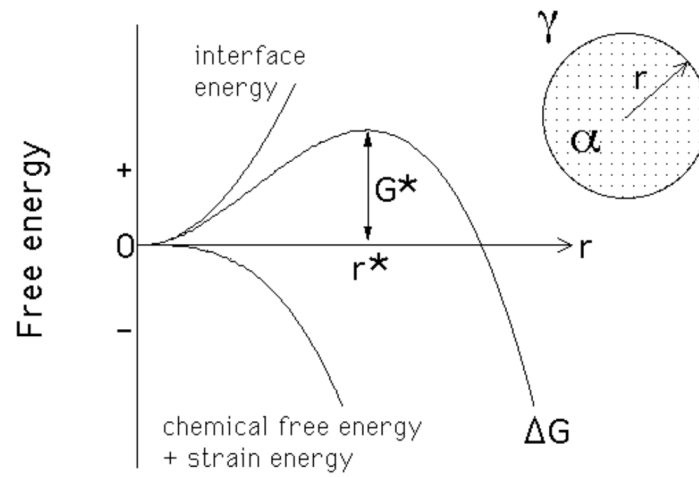


FIGURE 1.10: Variation in Gibbs Energy. Reprinted from [5]

The activation energy for the growth of nuclei can be calculated as -

$$G^* = \frac{16\pi\sigma_{\alpha\gamma}}{3(\Delta G_{CHEM} + \Delta G_{STRAIN})^2}$$

## Chapter 2

# Literature Survey

### 2.1 Introduction

In this attempt to cater requisite and current developments in microstructure evolution of alloys in metal additive manufacturing, the literature review [11] has been referred to get an understanding about the challenges that are currently prevalent in the community as well as lead this dissertation in desired direction in continuation to the previous work done on modelling this very phenomenon with CA. [6]

### 2.2 Literature Review

In the review [11], an attempt has been made by the authors to enlist the various microstructure characteristics as well as simulation methods that are employed for modelling microstructure of MAM process. These simulation methods were presented with their respective up and down sides which certainly helped in gauging the most suitable techniques to simulate this complex process. Specifically this paper addresses the microstructure characteristics in **Ti-6Al-4V** alloy. As suggested in the review, a lookup of future challenges prevailing in this area were carried out. This review concluded with a call for the need for large scale grain growth model in a moving melt pool for MAM process. Moreover, a generalised model of simulation is expected which will widen up its applicability to various MAM processes. Lastly, the development of these models needs to be guided on fundamental principles which will eventually simulate the complex grain

growth behavior in order to gain insights from the simulation.

MAM technologies can be bifurcated predominantly into two types namely, DED and PBF. In this dissertation an attempt has been made to model the microstructure for a DED process specifically WAAM process. A factor which distinguishes the above two types of AM processes is the cooling rate which is relatively lower for DED as compared to PBF process. Apart from this various other factors like different melt pool geometry, process parameters greatly affect the resultant microstructure. As can be evidenced that the uncertainty in relationship between PSP and microstructure of a product produced by AM presents a significant challenge for the control of quality and development of this manufacturing technique. Herein the numerical modelling of microstructure can aid in this linkage of mechanical properties with process parameters which govern the microstructural morphology of produced product and lend a hand in optimization and design of materials for desired applications. These AM processes result in manufactured parts with different defects and mechanical properties due to repeated melting and solidification across the layers. Some of the commonly observed characteristics in MAM processes are columnar grains, nucleation and epitaxial grain growth behavior and solid phase composition.

A conclusion that was made in the review[11] was that the present thermal welding models are not good enough to describe MAM process due to their inconsistencies in predictions of microstructures. Often **Ti-6Al-4V** is sorted to for analysis as all the three characteristics can be observed while MAM of these alloys. As the current research is based on deterministic models which are not appropriate enough to capture the uniqueness of MAM process like nucleation behavior, epitaxial growth, etc. Among the three, CA is presently used widely and was found to be quite suitable for simulations due to its lower computational cost compared to PF and a better physical basis compared to kMC method. In order to describe the grain growth of crystals, CA models can be utilised based on physics of dendrite kinetic tip for accuracy of simulation. Moreover, the PF models get limited by minimal time and length scales from physical theories. As is reviewed in the literature the melt pool geometry is quite important in order to achieve accurate microstructure evolution in MAM process. Although CA and kMC models can represent the evolution of microstructures due the thermal field because of this melt pool geometry but it is still a challenge for PF methods to work with varying temperature fields as relatively a large amount of calculation is involved in each time step for which often "constant temperature approximation" is sorted to simulate the microstructure evolution. This melt pool geometry aids in validation of simulation on a macro scale which eventually provides boundary conditions for meso and micro scale analysis. Apart from the above issues, the underlying rule

for nucleation is one of the open challenges in simulation of MAM process with the current simulations assuming epitaxial grain growth with no nucleation in melt pool can be physically applicable to a small number of MAM processes. Specifically in DED processes the grains are assumed to develop from substrate without any new nucleation which is close to what is observed in such process but certainly away from physical situation. So it seems quite reasonable to get boundary conditions of orientations of grains from experimental results rather than a random orientation assumption at the substrate with "no nucleation".

Competitive grain growth comes as a successive step to nucleation. Different methods simulate this phenomenon in a different manner like CA considers grain growth from kinetics perspective while PF considers it from thermodynamics perspective which eventually leads to deviation of the final microstructure from the observed one. In order to gauge the weightage of both the perspectives it appears as a rational step to increase the microstructure accuracy by experimental validation and database establishment for each recognized phenomenon.

In the above CA method, the dendrite tip kinetics result in grain growth usually presume local equilibrium which is not applicable in rapid solidification conditions. Moreover, it is a challenge with CA methods to appropriately represent the phenomenon of solute trapping as the interface often consists of single layer of cells wherein the solute fraction varies from 1 to 0 which certainly limits this technique to represent finer micro structural details. These finer details are often captured with PF model that is dependent on quantitative description of solid liquid interface.

As it is widely known that solid state transformations form an essential part of mechanical property evaluation in MAM, more recently density type simulations are incorporated for solid state transformations essentially in large scale coupled problems of additively manufactured component. Moreover, the validation of these simulations encounters its unique issues specifically that involving reconstructed EBSD which fails to capture higher order branches in microstructure and these experimental observations precisely do not account for true grain structure due to dynamic grain boundary migration in MAM process.

## Chapter 3

# Computational Approaches

Various different stochastic as well as deterministic methods are utilized in simulation of microstructure evolution in MAM process which involves a directional solidification along the printing direction. This whole process of microstructural modelling demands precise process modelling of additive manufacturing which serves as input to microstructural modelling in this process. The process of metal deposition in AM is similar to welding process which can be effectively modelled in order to model the process of metal deposition. As there can be thousands of passes in metal deposition process which resembles that of multi pass welding process which faces issues like inability to determine the exact location of weld pass during the process due to deformations that occur during the process. This whole issue of process modelling can be addressed with the aid of **Computational Welding Mechanics** which systematically models all the aspects of welding process.

The modelling of microstructure in MAM process can be achieved with various methods as -

1. Cellular Automata(CA) Method
2. Phase Field (PF) Method
3. Monte Carlo Method
4. Needle-Network Method

### 3.1 Cellular Automata Method

CA is a kind of computational technique wherein a discrete group of cells are evolved by invoking certain rules in an iterative manner on each cell. Although, these rules on cellular level are simpler to invoke but these rules collectively are capable to represent complex behavior during simulation. In contrast to general dynamics model, CA is not rigorously defined by physical equation, instead by rules pertaining to various models[16]. In this technique, the local rules invoked with neighbors are often deterministic or stochastic in nature.

Looking back these 25 years, CA has successfully been used to simulate the evolution of microstructure like static recrystallization[15], dynamic recrystallization[12] and the grain growth behaviors[3]. The first CA model to incorporate the solidification behavior was developed in the 1990s[13]. The classic cellular automata technique can be characterised as :

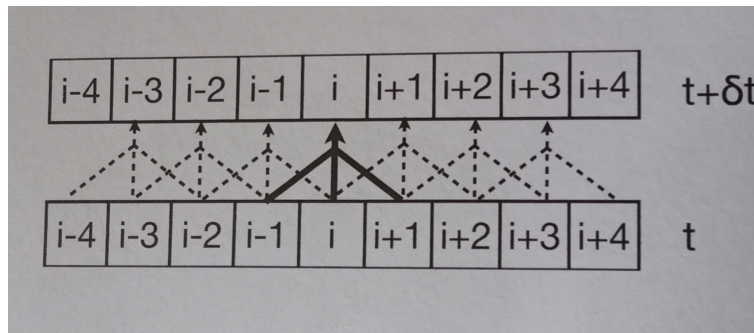


FIGURE 3.1: Rules for one-dimensional Cellular Automata(Picture Courtesy : [10])

1. Discrete in Space
2. Homogeneous
3. Discrete States
4. Discrete in Time
5. Synchronous updating
6. Deterministic Rules
7. Spatially local rule
8. Temporally local rule

Among all the above characteristics , **synchronous updating of all the cells** is a feature which makes this techniques different from Monte Carlo technique.

In case of 2D CA,the behavior of automata is dependent on local rules which in turn depend upon the representation of neighborhood for each cell. Conventionally there are two of the choices for local environment for a square lattice i.e. the **Von Neumann** environment and the **Moore** environment .The Von Neumann neighborhood consists of four neighbors of the concerned cell whereas Moore neighborhood consists of eight neighbors surrounding the cell as can be seen in the figure below.

In context of material science , a simple simulation as discussed in [8] for modelling recrystallization process using CA has been simulated within MATLAB framework in order to gain understanding how CA is implemented in physical processes with focus on mainly three phenomenon :

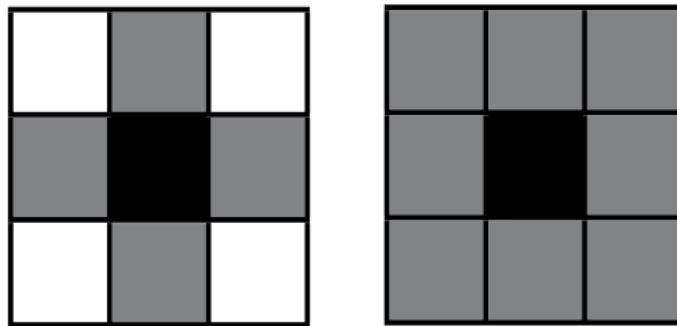


FIGURE 3.2: Neighborhood Configurations in CA(Picture Courtesy : [10])

tallization process using CA has been simulated within MATLAB framework in order to gain understanding how CA is implemented in physical processes with focus on mainly three phenomenon :

1. Nucleation of Grains
2. Growth of Grains
3. The slowing of growth owing to the impingement of cells

At the initial stage all the cells were marked as state 0 (not recrystallized) and a random number of cells were marked with non zero states to model the nucleation of grains. A simple rule for the growth of these non zero states or embryos are defined as if the activity defined as sum of states of recrystallized neighbors corresponding to Von Neumann or Moore's neighborhood is greater than 1 at any time step then the central cell would be considered recrystallized (i.e. change state to non zero value) at step  $t+1$  and take on the identity of a grain that extends



to its neighborhood. In order to model the decrease in growth due to impingement the rate of nucleation is varied from the initial rate of nucleation. The simulated results are shown below

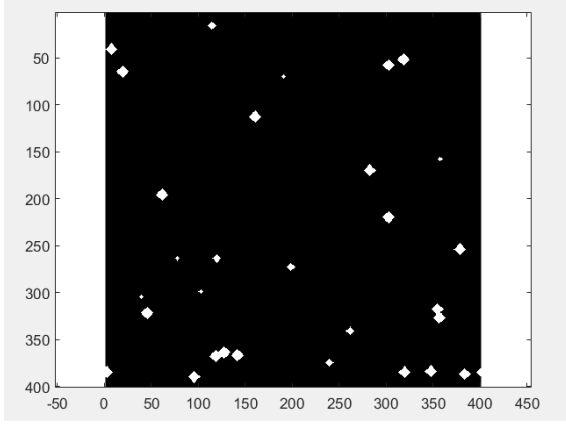


FIGURE 3.3: Randomly Nucleated Grains

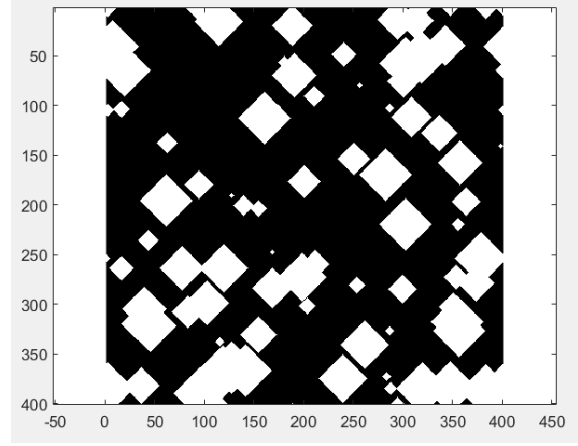


FIGURE 3.4: Growth of Grains along with Residual Nucleation

### 3.2 Phase Field(PF) Method

In phase field methods, the entire microstructure or the matrix along with precipitate and interface is represented by a single order parameter  $\phi$ . Let's say for simplicity in case of precipitate growth in a matrix,  $\phi = 0$  represents the matrix while  $\phi = 1$  represents the precipitate but in here the jump from  $\phi = 0$  to  $\phi = 1$  creates a problem for computation of evolution so a finite width of interface separating the precipitate and matrix is taken into account in order to describe the evolution of the system with the help of single parameter. The set of values that the parameter takes over the entire microstructure comprise a **phase field**.

The evolution of the microstructure with time is assumed to be proportional to the variation of free energy functional with respect to the order parameter :

$$\frac{\partial \phi}{\partial t} = M \frac{\partial g}{\partial \phi} \quad (3.1)$$

wherein  $M$  is the mobility and the term  $g$  accounts for the free energy functional. At constant  $T$  and  $P$ , it takes the form

$$g = \int_V [g_0 \phi, T + \epsilon (\nabla \phi)^2] dV$$

Here, the second term describes the interfacial energy whereas the first term accounts for the sum total of free energies of precipitate and matrix.

Often two types of parameters were observed in material modelling one that is conserved and another that is not conserved.

### 3.2.1 Cahn-Hilliard Treatment of Spinodal Decomposition

In solutions that evolve towards clustering, there is a possibility for a phase to become unstable due to infinitesimal perturbations in chemical composition. The free energy of heterogeneous solid solution can be classified into three parts i.e. a part which consists of free energy of homogeneous solution in isolation, the interfacial region which comes into existence due to the difference in neighboring environment as compared to homogeneous solution and the last part of energy gets in due to the lattice strains (**coherency strains**) which are caused due to variations in chemical composition. So the Gibbs free energy functional can be given as :

$$g_T = \int_V \left[ g(c_0) + k_2 \frac{d^2 c}{dx^2} + k_3 \frac{dc^2}{dx} \right]$$

In particular, the interface is not tracked but is given implicitly by the chosen value of the order parameter as a function of time and space.

## 3.3 Monte Carlo Methods

This technique was initially developed to evaluate integrals numerically especially multi-dimensional integrals where random volumes are sampled over the region of interest by tracking which points are sampled within the volume and which are left leading to estimation of integral as a fraction of the region encompassing the integrand function. But eventually incorporating a large number of trials can lead to an acceptable convergence of the integral which adds to the computational burden of its implementation.

As discussed by Metropolis in his 1953 paper [1] wherein the configuration space is sampled in a manner so that the state  $\alpha$  happens in the sampling with a probability  $\rho_\alpha$  which is often known as **Metropolis Algorithm**. This algorithm allows us to distribute states corresponding to their correct probabilities which helps in determination of average outcome from these states. This approach begins with the selection of a configuration space of states often known as trajectory

of that space, upon starting the simulation with a certain configuration, a decision is made whether to add a new configuration to the configuration space by computing the probability of trial move relative to original configuration and comparing it with a certain threshold.

### 3.3.1 Ising Model

Ising model gives a classic implementation of Monte Carlo Method. This model although being fairly simpler describes magnetism, phase transformations, etc. As discussed in Swapnil's dissertation [6] the model was implemented with the similar configuration space wherein the spin states (0 or 1) are randomly assigned to all the points on a square lattice. A trial move is invoked by selecting a site randomly and calculating its bond energy with the concerned neighborhood configuration of 4 or 8 neighbors surrounding the site in a lattice. Eventually incorporating Glauber Dynamics or Kawasaki Dynamics in order to complete the trial move after which the new bond energy is calculated relative to previous configuration so as to accept or reject this state based on Metropolis function.

The bond energy is computed as an aggregate of all the bond energies for a randomly selected site with its neighborhood configuration which is computed as following :

$$\gamma(s_i, s_j) = \begin{cases} 1 & \text{for } s_i = s_j \\ 0 & \text{for } s_i \neq s_j \end{cases} \quad (3.2)$$

In order to compute new bond energy, Glauber Dynamics or Kawasaki Dynamics can be incorporated. In Glauber Dynamics, a random spin is assigned to current site in order to calculate new bond energy where in Kawasaki Dynamics, a random neighbor is selected from the neighborhood to swap the spin with current site to calculate the new energy. Glauber dynamics is non conservative in nature while Kawasaki dynamics is conservative i.e if the system simulation is started with  $n_1$  number of spin 1 and  $n_2$  number of spin 0. Then using Kawasaki dynamics will end up the simulation with same number of spins which is expected attribute of a closed system.

The Metropolis function that provides with the threshold probability which acts as a acceptance criteria for the new configuration is given by :

$$P(\Delta E) = \begin{cases} 1 & \text{if } \Delta E \leq 0 \\ e^{\frac{-\Delta E}{kT_s}} & \text{if } \Delta E > 0 \end{cases} \quad (3.3)$$

Here  $\Delta E$  is the difference in bond energies of original configuration and new configuration which is calculated as

$$E = \sum_{k=1}^n \gamma(s_i, s_j) \quad (3.4)$$

in a n neighbor environment. Moreover, in equation 3.3  $k$  is the Boltzmann constant and  $T_s$  is the simulation temperature which controls the thermal fluctuations in a system. In an attempt to neglect the temperature effects and solely consider the changes in bond energy, this product  $kT_s$  is assumed to be constant equal to 0.0001.

When the lattice is traversed completely by making enough trial moves, it is called one Monte Carlo Step (MCS) and the simulation is run for 1000 steps. The configuration state at initial time and after certain time steps can be pictorially depicted as :

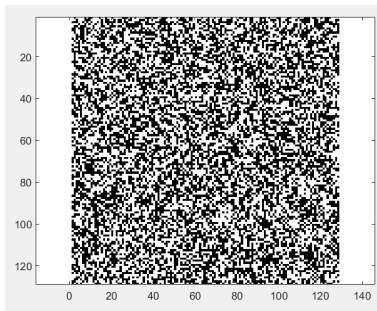


FIGURE 3.5: Simulation at initial time

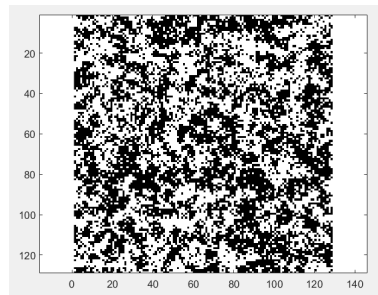


FIGURE 3.6: Simulation at time  $t_1$

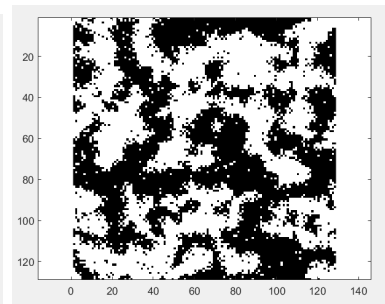


FIGURE 3.7: Simulation at time  $t_2$

FIGURE 3.8: Simulation of Ising Model (Here  $t_2 > t_1$ )

Moreover, in this simulation a modification is also implemented which as discussed in [lesar] in order to speed up the simulation by making a trial move, checking the feasibility of new configuration after swap and its implementation is carried successively for each random site rather than making just a trial move over the entire Monte Carlo Step i.e. just for the first random choice one starts with the initial configuration and then successively modifies the configuration with every random site.

### 3.3.2 Kinetic Monte Carlo

This method is fundamentally Monte Carlo Method applied to rates. Certain class of problems demand for a relationship between Monte Carlo Time and actual time which can be effectively addressed by kinetic monte carlo simulations. This technique has been proved in various rate controlled processes like diffusion, chemical reaction, etc.

The fundamental idea behind kinetic Monte Carlo simulations is the association of probability of an event with its average rate of occurrence. If more than one event occur in a system then at any time the probability of a event relative to all other events is proportional to its rate relative to the rates of other events.

In kinetic Monte Carlo method, the first step is to enlist all the possible events that can occur in a system with their corresponding rates of occurrences. The algorithm that is followed in these simulations can be summarised as :

1. At a given time  $t$ , all the events that could happen in a system are determined and their corresponding rates are added up in order to calculate activity as :

$$A(t) = \sum_{k=1}^M r_k(t) \quad (3.5)$$

wherein  $M$  is the number of events that can occur at that specific time.

2. The probabilities of each such are calculated by dividing the corresponding rate with  $A(t)$
3. A list of events is to be created weighted by their probabilities.
4. In order to make a decision which event will occur , a random number  $\mathbb{R}$  between  $(0, 1)$  is picked such that

$$\frac{\sum_{k=1}^{m-1} r_k}{A} < \mathbb{R} < \frac{\sum_{k=1}^m r_k}{A} \quad (3.6)$$

wherein  $m$  is the concerned event.

5. the chosen event is enacted based on above decision leading to new configuration of the system
6. Then the time is advanced by  $\Delta t$  which is computed as :

$$\Delta t = \frac{1}{A(t)} * \ln((R)) \quad (3.7)$$

7. The above steps are invoked once again in order to reach a decision .

In an attempt to understand the implementation of this method, a simulation is done to represent point defects in Si crystal wherein for simplicity migration of interstitial and vacancies are only considered by ignoring clustering of these defects.

It is a well established observation that when a vacancy and interstitial come sufficiently close to each other , the extra interstitial atom fills in the vacant lattice site and only perfect Si lattice will remain .

For simulation of this process , a paper reporting migration properties [2] has been considered wherein

$$\text{jump rate}(T) = w = w_d e^{\frac{-E^m}{k_B T}} \quad (3.8)$$

where  $w_d$  is the defect jump rate prefactor and  $E^m$  is the migration activation energy . So in the simulation , there are 3 possible processes:

1. A vacancy jumps by  $2.35 \text{ \AA}$  in a random direction
2. An interstitial jumps by  $2.35 \text{ \AA}$  in a random direction
3. If a vacancy and interstitial are within  $4 \text{ \AA}$  from each other, they will immediately recombine and vanish from the system.

As the simulation is done at a constant temperature, the algorithm for the simulation can be summarized as :

1. (a) Set the time  $t = 0$  . Set initial positions for all N defects  $x_j$  and their types  $t_j$ . Set the temperature T and recombination radius  $r_{rec} = 4.0 \text{ \AA}$ . Set  $N_{iter} = 0$  and select  $N_{itermax}$ .
- (b) Go through all defects and for each defect find whether any defect of opposite type is closer than  $r_{rec}$  to it. If so, remove both from the tables  $x_j$  and  $t_j$ , set  $N = N - 2$ .
- (c) Calculate the jump rate for interstitials from T (Melting point of Si 1685 K) :  
 $w_i = w_i e^{\frac{-E_i^m}{k_B T}}$  and same for vacancies  $v$ .
2. Set  $r_j = w_d$  where  $d = i$  or  $d = v$  depending on the defect type  $t_j$ .
3. Calculate the cumulative function  $R_j = \sum_{k=1}^j r_k$  for all j and denote  $R = R_N$ .

4. Get a uniform random number  $u \in [0, 1]$
5. Find the defect to move  $j$  out of the lattice by finding  $j$  for which
 
$$R_{j-1} < uR \leq uR_j$$
6. Carry out jump  $j$  by displacing defect  $j$  in a random direction by  $2.35 \text{ \AA}$
7. For defect  $j$ , find whether any defect of the opposite type is closer than  $r_{rec}$  to it. If so, remove both from the tables  $x_j, t_j$  and  $r_j$ , set  $N = N - 2$ .
8. Get a uniform random number  $u \in [0, 1]$
9. Update the time with  $t = t + \Delta t$  where :
 
$$\Delta t = -\frac{\log u}{R}$$
10. Set  $N_{iter} = N_{iter} + 1$  and continue the above procedure till  $N_{iter} < N_{itermax}$

Implementing the above algorithm, the results of the simulation at different stages of a iteration are shown as :

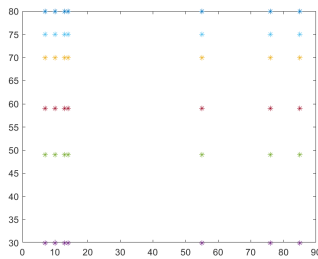


FIGURE 3.9: At initial time

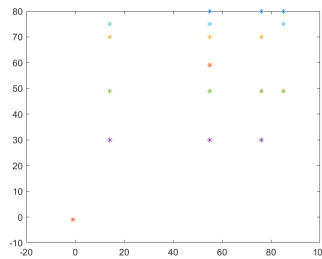


FIGURE 3.10: After Re-combination

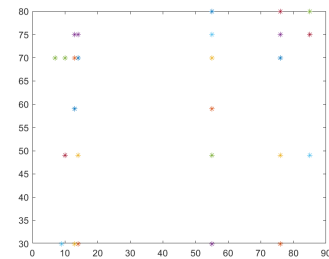


FIGURE 3.11: Remaining interstitials and vacancies

FIGURE 3.12: System Configuration in First Iteration

### 3.4 Needle Network Method

Recently, a new technique of Dendritic Needle Network(DNN) has been introduced in [7] as a work around to limitation of phase field method. This models captures higher order dendritic branches which in effect develop their own diffusion field and eventually interact with one another. Laplacian growth theory [4] is implemented to compute growth dynamics of these needle crystals. Two conditions are considered in computation of tip velocity and radius of curvature of these dendritic needles which are firstly the standard solubility condition on the scale of dendrite tip and an additional flux balance on a outer scale .Different from PF method , DNN extends its focus to grain scale by ignoring its focus on tip scale solid liquid interface by certain loss of accuracy thereby eventually tries to bridge in the scale gap between PF and CA methods. A simplified version of needle network model has also been applied to study the epitaxial growth behavior of columnar grains and predict the texture in MAM process as discussed in [9].



# Bibliography

- [1] Metropolis et al. “Equation of state calculations by fast computing machines”. In: *Journal of Chemical Physics*, 21, 1087-1092 (1953).
- [2] Tang et al. “Intrinsic point defects in crystalline silicon: Tight-binding molecular dynamics studies of self-diffusion, interstitial-vacancy recombination, and formation volumes”. In: *Phys. Rev. B.* 55 14279 (1997).
- [3] Zinoviev et al. “Evolution of grain structure during laser additive manufacturing. Simulation by a cellular automata method”. In: *Materials Design* 106:321-329 (2016).
- [4] V. Hakim B. Derrida. “Needle models of Laplacian growth”. In: *Physical Review A* 45(12):8759-8765 (1992).
- [5] Prof. H.K.D.H. Bhadesia. *MPhil Course on Materials Modelling*.
- [6] Swapnil Bhure. “Micro structure Modelling in Additive Manufacturing (Dissertation)”. In: *Birla Institute of Technology and Science, Pilani* ((2019)).
- [7] A. Karma D. Tournet. “Multi-scale needle-network model of complex dendritic microstructure formation”. In: *IOP Conference Series: Materials Science and Engineering* 33 (2012).
- [8] H. W. Hesselbarth and I. R. Gobel. “Simulation of recrystallization by cellular automata”. In: *Acta Metallurgica et Materialia*, 39, 2135–2143 (1991).
- [9] Y. Zhao W. Xiong A. To J. Liu Q. Chen. “Quantitative Texture Prediction of Epitaxial Columnar Grains in Alloy 718 Processed by Additive Manufacturing”. In: *Proceedings of the 9th International Symposium on Superalloy 718 Derivatives: Energy, Aerospace, and Industrial Applications*, Springer, pp. 749-755 (2018).
- [10] Richard LeSar. *Introduction to Computational Materials Science : Fundamentals to Applications*. Cambridge University Press, (2013).

- [11] Zhou X. Brochu M. Provatas N. Zhao Y. F. Li J. “Solidification microstructure simulation of Ti-6Al-4V in metal additive manufacturing: A review”. In: *Additive Manufacturing*, 31, 100989 ((2020)).
- [12] Z.X. Guo M. Qian. “Cellular automata simulation of microstructural evolution during dynamic recrystallization of an HY-100 steel”. In: *Materials Science and Engineering: A* 365(1-2):180-185 (2004).
- [13] C.-A. Gandin M. Rappaz. “Probabilistic modelling of microstructure formation in solidification processes”. In: *Acta Metallurgica et Materialia* 41(2):345-360 (1993).
- [14] Easterling K. E. Sherif M. Y. Porter D. A. *Phase transformations in metals and alloys*. CRC Press, (2018).
- [15] D. Raabe. “Mesoscale simulation of recrystallization textures and microstructures”. In: *Advanced Engineering Materials* 3(10),745 (2001).
- [16] S. Wolfram. “Computation theory of cellular automata”. In: *Communications in mathematical physics* 96(1):15-57 (1984).